Chlorophyll-A variability in the southern coast of Java Island, Indian Ocean: corresponding to the tropical cyclone of Ernie

U Efendi[1], A Fadlan[2], A M Hidayat[1]

[1] Under Graduate Program of Meteorology, State College of Meteorology Climatology and Geophysics, Indonesia
[2] Lecturer, Department of Meteorology, State College of Meteorology Climatology and Geophysics, Indonesia

E-mail: usman.efendi@bmkg.go.id

Abstract. Tropical cyclone is an atmospheric phenomenon formed above warm ocean in a tropical region. Generally, tropical cyclone gives negative impact, such as extreme rainfall, strong winds, and extreme wave height. On the other hand, however, tropical cyclone gives positive impact on triggering the ocean fertility by induced chlorophyll-a concentration caused by vertical mixing and upwelling in the ocean. Related to this, a study has been conducted to determine the concentration of chlorophyll-a after the occurrence of Ernie cyclone in Indian ocean near western part of Australia and along the southern coast of Java island. The data that used in this study is daily wind speed data from 5 - 11 April 2017, daily average data of SST from 5 - 11 April 2017, and 8-day composite data of chlorophyll-a data from Aqua-MODIS satellite. The analysis of chlorophyll-a concentration showed a slow response of ocean fertility increment in the southern coast of Java island. Chlorophyll-a concentration along the cylone trajectory prior to the cyclone was in the range of 0.08 mg/m^3 – 0.15 mg/m^3 and significantly increased up to 88%–100% in a week after the occurrence of cyclone. On the next third and fourth weeks after cyclone, the concentration of chlorophyll-a along the cyclone trajectory decreases gradually. Meanwhile its sea surface temperature decreased significantly, especially in areas where cyclone had passed.

1. Introduction

Tropical cyclone is one of the most destructive meteorological activities on earth which commonly associated with strong wind, heavy rain, and induce large wave in the ocean. Besides numerous calamities caused by the activity of cyclone, studies have shown that cyclone events lead to the increase of nutrient and phytoplankton increment in the water column, which depend on its translation speed and intensity [1]. The energy of cyclone penetrates into the ocean cause strong entrainment and mixing [2][3][4]. This energy play a substantial role on the changes of upper ocean environment and its physical characteristic [5][6][7][8][9][10][11].

The maximum cooling observed on the right of the cyclone track in northern hemisphere and to the left of the track in southern hemisphere when the cyclone moves rapidly, while the maximum cooling occurs well near or on the track for slowly moving cyclone [12]. Suetsugu et al. [13] revealed that atmosphere-ocean parameter dependence, such as storm strength level, storm translation speed, and upper ocean thermal structure, influence the cooling process of sea surface temperature. As conclusion,

they described that the strong and slow moving cyclone causes maximum cooling of 5 °C in the cyclone wake.

According to Lin and Wu [14], the emergence of cyclones, which decrease sea surface temperature (SST), lead to subsequent changes in nutrient concentrations and the uptake of nutrients (upwelling) by phytoplankton, which significantly affects chlorophyll-a (Chl-a) and depth-integrated primary productivity (IPP). Upwelling brings rich nutrient water from sub surface to the euphotic zone where there is abundant light for photosynthesis but often lack of nutrients [15]. The chlorophyll-a increment may occur along the cyclone track or in nearby coastal region. Hung et al. [16] observed that the increase of chlorophyll-a concentration not only at the surface, but also above thermocline. After the occurence of typhoon Fengwong, they found that the in situ measured on the subsuface chlorophyll-a concentration was 50% higher than the imagery analysis using moderate-resolution imaging spectroradiometer (MODIS) data, therefore the depth of euphotic zone also increased.

Hong and Sohn [17] and Kim et al. [18] declares that upwelling, caused by Ekman pumping, was active when cyclone passes over a specific sea surface and the cold-water injection into the surface layer from a deeper layer continues to spread horizontally outwards. This mechanism considered as one of the main factors supporting vertical mixing, and, as a result changes on various factors which may last for quiet long period [19]. On April 2017, a tropical cyclone, named Ernie, was form at latitude 13.30°S and longitude 110.8°E in the Indian ocean. This cyclone grew intensively until it was declared as tropical cyclone category 4 based on Saffir-Simpson hurricane scale with a maximum wind speed of 130 knots. Although Ernie cyclone did not pass Indonesia but the distance between this cyclone and southern coast of Java was quite close.

During cyclone period, the measurement of biological and physical parameter onboard ship is very arduous due to severe weather conditions as one of the cyclones impact. Krishna and Song [20] stated that the development of multi satellite remote sensing, especially microwave remote sensing, in combination with numerical simulation, provide powerful tools for further understanding the upper ocean changes induced by cyclone. Hence, the development of multi-satellite remote sensing provides worthwhile equipment to analyze the upper ocean dynamic changes. Most studies of cyclone effects on chlorophyll-a have focused on the concentration of uptake nutrient around the cyclone treajectory. However, the impacts of cyclone on the coastal region remain unclear. Therefore, this study examines the effect of Ernie cyclone on the concentration of chlorophyll-a on the southern coast of Java island and along the cyclone track using very high-resolution satellite imagery.

2. Data and Methodology

2.1 Research Site

The study was conducted along the track of Ernie cyclone and along the southern coast of Java island (Fig. 1). Analysis of the impact of tropical cyclones on aquatic area was carry out in two main areas: along the emergence of Ernie cyclone (cyclone track, A1) and along the coastal region in the southern coast of Java (A2), which precisely located at the coordinates of 7° 58’ 45’’ S 109° 43’ 15’’ E. Coastal region (A2) put into important consideration because it is assumed as the most potential region of fishing.

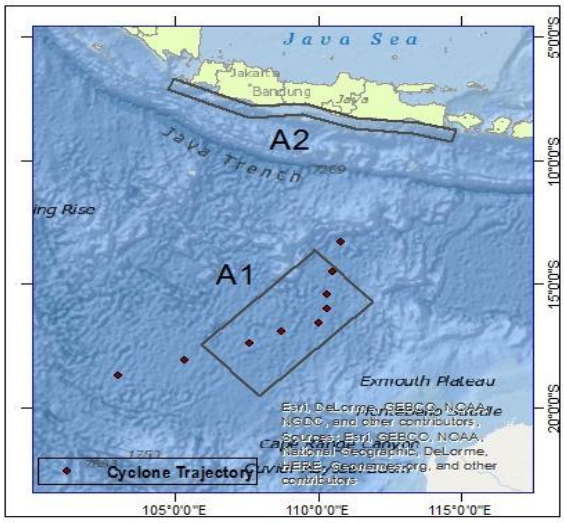

Figure 1. The research site focused on 2 regions depicted as A1 and A2. A1 showed an area of cyclone trajectory, while A2 was a coastal region on the southern part of Java.

2.2 Data Sources

2.2.1 Cyclone information for Southern Indian Ocean. The tropical cyclone data that used in this study is provided by the Joint Typhoon Warning Center (JTWC), from 6 - 10 April 2017, in the geographical range of 100°E-115°E and 5°-20°S (Fig. 1). Ernie cyclone was active in the southern coast of Java island, Indian ocean for about 5 days (Table 1). The table contain several information related to the cyclone, such as the name of tropical cyclone, the coordinates location of its center, observed time (about 6-h interval), and maximum sustained wind speed. Tropical cyclone Ernie is the third tropical cyclone occurs in the southern Indian ocean in 2017. The maximum wind velocity of tropical cyclone Ernie is considered to be the highest amongst other tropical cyclones, reached up to 130 knots. Ernie cyclone was declared as a tropical cyclone category 4 on the Saffir-Simpson hurricane scale. Based on tropical cyclone data obtained from www.weather.unisys.com, the coordinates and wind velocity of tropical cyclone Ernie can be seen in the following table 1.

Tabel 1. The detailed data about the condition at pre-cyclone periods, at the cyclone event, and post-cyclone. The data contains information about times of occurrence, coordinate location of the cyclone, maximum speed, and also its category based on Saffir-Simpson hurricane scale.

Dates	Hour (UTC)	Latitude	Longitude	Maximum wind speed (knots)	Category
6/April/2017	06	-13.3	110.8	35	Tropical storm
6/April/2017	18	-14.5	110.5	40	Tropical storm
7/April/2017	06	-15.4	110.3	95	Tropical cyclone (2)
7/April/2017	18	-16	110.3	130	Tropical cyclone (4)
8/April/2017	06	-16.6	110	95	Tropical cyclone (2)
8/April/2017	18	-16.9	108.7	90	Tropical cyclone (2)
9/April/2017	06	-17.4	107.6	85	Tropical cyclone (2)
9/April/2017	18	-18.1	105.3	55	Tropical storm
10/April/2017	06	-18.7	103	40	Tropical storm

Source: http://weather.unisys.com/hurricane/

2.2.2. Sea surface temperature (SST). The value of daily average SST is derived from NASA Jet Propulsion Laboratory (JPL) Multi-scale Ultra-High-Resolution Sea Surface Temperature (MUR SST)

with specific resolution of 1 km. SST data can be obtained online through https://mur.jpl.nasa.gov/DownloadDataText.php. The daily average of sea surface temperature was displayed in the form of spatial distribution map from 5 - 11 April 2017.

2.2.3. Sea surface wind. The blended sea winds contain globally gridded, high resolution ocean surface vector winds and wind stresses on a global 0.25° grid. The spatial variation of wind force produces a consequent variation in the corresponding with Ekman transport in the surface layer, causing convergence and divergence in different areas. This leads to "Ekman pumping" [21]. Wind data is obtained from the Advanced Scatterometer (ASCAT) sensor on the METOP satellite. The wind data used in this research is daily average data of surface wind. The data measured at a height of 10 meters above sea level and has a grid resolution of 0.25° x 0.25°. The data can obtain online through ERDDAP server website (http://coastwatch.pfeg.noaa.gov/erddap/index.html). Furthermore, the wind speed and direction were calculated according to the following formula:

$$Wind\ speed = \sqrt{x\ wind^2 + y\ wind^2} \quad (1)$$

$$wind\ direction = 90 - \left(\left(\frac{180}{\pi} * ATAN2\left(\frac{x_{wind}}{y_{wind}}\right)\right)\right) \quad (2)$$

Where x wind is zonal wind (knots) and y wind is meridional wind (knots) [22]. The calculated data were displayed in the form of spatial distribution of daily average wind speed and direction.

2.2.4. Chlorophyll-a concentration. There are several ways to analyzed the variability of chlorophyll-a concentration in the ocean. Susilo and Hardianti [22] used sensor of the Visible Infrared Imaging Radiometer Suite (VIIRS) on the Suomi National Polar-orbiting Partnership or Suomi NPP satellite. Nuris et al. [23] declared that the results of VIIRS - NPP sensor and Moderate Resolution Imaging Spectroradiometer (MODIS) had the same pattern, however the estimation of chlorophyll-a concentration from the MODIS sensor was higher than VIIRS -NPP sensor. Therefore, this study used chlorophyll-a concentration data from MODIS sensor on the Terra satellite /Aqua-MODIS. Spatial distribution and temporal variation of chlorophyll-a concentration is based on the 8-day composite data. The used of this method is due to unavailability data of chlorophyll-a concentrations since the cyclone trajectory area is mostly covered by cloud. Chlorophyll data can be obtained online through ERDDAP server website (http://coastwatch.pfeg.noaa.gov/erddap/griddap/erdMH1chla8day.html). The chlorophyll data were presented in the form of spatial distribution and hovmoller diagram. The spatial map of chlorophyll-a was made within 3 times period, 30 March - 6 April 2017, 7 – 14 April 2017, and 15 – 22 April 2017. The hovmoller diagram was created to determine the spatio-temporal variation of chlorophyll-a along the southern coast of Java Island beginning at early February 2017 to early June 2017.

2.3 Data Analysis

Distribution of sea surface temperature, daily average wind, and 8-day composite data of chlorohyll-a was analyzed using GrADS 2.02.oga.2 software. The analysis was conducted to determine the pattern of sea surface temperature, wind speed and direction, and also the variability of chlorohyll-a during pre-cyclone period, at cyclone event, and post cyclone period. The pattern of each data then analyzed in two research areas, A1 and A2, in order to comprehend the effects of ernie cyclone toward the variability of chlorophyll-a concentration along the southern coast of Java island. The variability of chlorophyll-a on the southern coast of Java island (A2) before and after the occurrence of Ernie cyclone then analyzed using Ocean Data View (ODV) in order to create a hovmoller diagram.

3. Result and Discussion

3.1. Computation of daily-average surface wind from METOP-ASCAT

Surface wind, which blow over the ocean, is parameter that has considerable impact due to the activity of tropical cyclone Ernie. Significant pressure difference between the cyclone center and its surrounding areas made the wind speed in that area was quite high. When cyclone happens, wind velocity generally increases along the cyclone trajectory, but tends to be weak at the center of the cyclone [22]. Tropical cyclone also leads to the increase of wind speed and retard the current movement [1]. Surface wind conditions around the area of Ernie cyclone and southern coast of Java island were represented in Fig. 2. Wind speed shown in the daily-average value from ASCAT sensor so that the value was lower when compared to the maximum value of wind velocity stated in table 1. This different occurred because the wind speed value shown by ASCAT sensor is the average value not the maximum value as what stated on table 1.

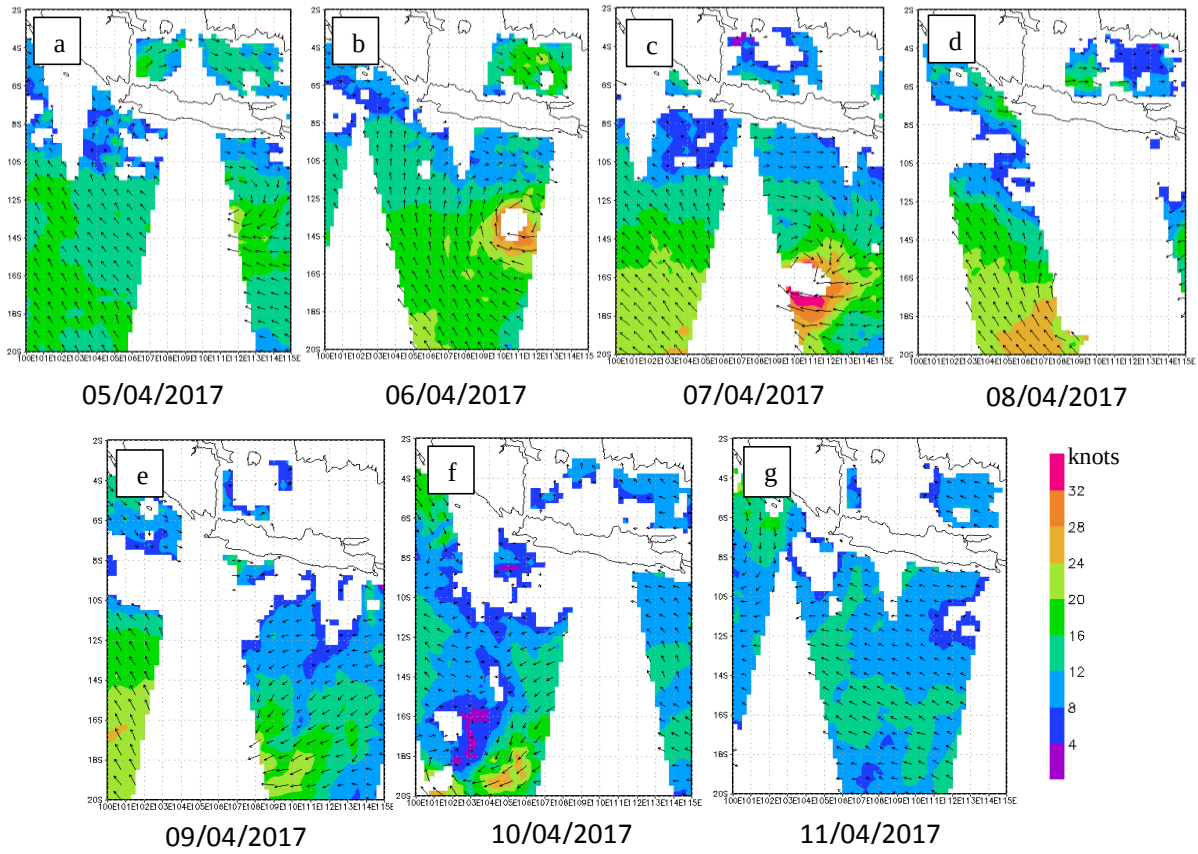

Figure 2. The daily-average data of surface wind from pre-cyclone period, a) 5 April 2017, to the post-cyclone period of tropical storm, g) 11April 2017, in the southern coast of Java island. Wind speed is expressed in knots.

Generally, the daily-average of surface wind direction in April is dominated by easterly wind pattern [24]. However, surface wind direction at the initial phase location of cyclone-formation until the occurrence of Ernie cyclone was dominated by westerly wind patterns. This indicated that the tropical cyclone phenomenon changed the daily-average wind direction in April. As consequences, the changes in the surface wind direction will also impact on the changes of the sea surface current direction [25][26].

The daily-average wind speed on 6 April 2017 in the southern coast of Java (A2 region) was quite high, within the range of 8 - 20 knots. At that time, the location of Ernie storm was quite close to the A2 region, therefore it induced large pressure gradient between A1 and A2. The bottom line is, the higher

value of air pressure gradient, the greater the wind speed occured as the impact of cyclone. Tropical cyclone activity continued to develop and grow, reached its peak, and classified into 4th scale tropical cyclone in the night of 7 April 2017. In this condition, the surface wind speed in A2 region decreased slightly, however the value of wind speed in A1 region increased up to more than 32 knots. Analysis on the streamline showed there was a divergence in the southern region of Banten province caused a decrease in wind speed in A2 region.

A day after Ernie cyclone reached its peak intensity, the condition of the surface wind could not be observed, regarding the inability of ASCAT sensors to record the conditions in A2 region due to the dense cloud coverage. But in general, the condition of surface wind decreased in the range of 6-16 knots along with weakening activity of Ernie cyclone until it was started to decay on 10 April 2017. The weakening of surface wind speed continued because the distance of cyclone track to the A2 region was getting further. As time goes by, the activity of Ernie cyclone became weaker and therefore triggered the weakening of air pressure gradients between the two areas.

Meanwhile, the wind direction after the occurence of Ernie cyclone experienced a significant change in the A2 region. On 8 - 9 April 2017, the southern coast of Java island was still dominated by westerly wind pattern as the impact of Ernie cyclone, but on 10 - 11 April 2017 when the cyclone started to decay, the daily-average wind direction changed again into easterly wind pattern. As the wind blows from east to west, the direction of the current will flow to the south by the Ekman transport, so that the sea-surface current would flow away from A2 region and there would be a vacuum of sea water along that region. This condition triggered entrainment of colder water from below which is accompanied by an enhancement of primary production moved to the upper oceanic layer, commonly known as upwelling mechanism. Generally, sea water temperatures formed below tend to be cooler than that on the surface layer, therefore the changes in surface wind patterns will also affect sea surface temperature patterns.

3.2. Response of sea surface temperature

Temporal variation and spatial distribution of sea surface temperature represent the water column conditions before the decayed of tropical cyclone (Fig. 3). One of the factors that triggered the occurrence of tropical cyclone in a certain region is the warmer of Sea Surface Temperature (SST) on that region compare to its surrounding. The formation of tropical cyclones around the equator generally occurs at temperatures above 26.5^{o}C [27][28][29] and in the region with latitude of 35^{o}, cyclone also occurred at the same temperature [30]. Sea surface temperatures in A1 and its surrounding areas prior to the occurrence of tropical cyclones (April, 5 – 6 2017) showed a relatively high value of SST between the range of 30 - 32^{o}C. The high sea surface temperatures led to the formation of a low-pressure area which triggered the occurrence of tropical cyclone Ernie [22].

A1 region showed a significant decrease in sea surface temperature during the occurrence of tropical cyclone events which was 7^{o}C lower than the previous day. The sharp drop in the sea surface temperature on the tropical cyclone trajectory caused by Ekman pumping mechanism induced upwelling and the vertical mixing process. This mechanism caused the cold water injection into the surface layer from a deeper layer continues to spread horizontally outwards. This horizontally spreading is considered as one of the main factors supporting vertical mixing, and, as a result, continues changes in various factors may last for some time [17].

Tropical cyclone creates a whirlpool that rotates clockwise in the southern hemisphere and anti-clockwise in the northern hemisphere. This vortex caused a change in ocean surface currents. In southern hemisphere, the direction of the ocean currents rotated to the left (stayed away from the center of the cyclone) due to the Ekman transport mechanism, resulting an emptiness of sea water at the center of the cyclone. This emptiness replaced by the rising of cold water mass from the deeper layer of the sea. Therefore, sea surface temperature showed a relatively low value between the range of 24 - 27^{o}C during the cyclone period and maximum cooling happened when Ernie cyclone was on its peak intensity. This cold pool slowly decreased after the passage of Ernie cyclone which accompanied by the weakening of the cyclone activity. This clearly indicated that the maximum cooling and hence the cold pool, at the

left side of cyclone track, was generated by the cyclonic wind-stress curl and the associated upward Ekman pumping.

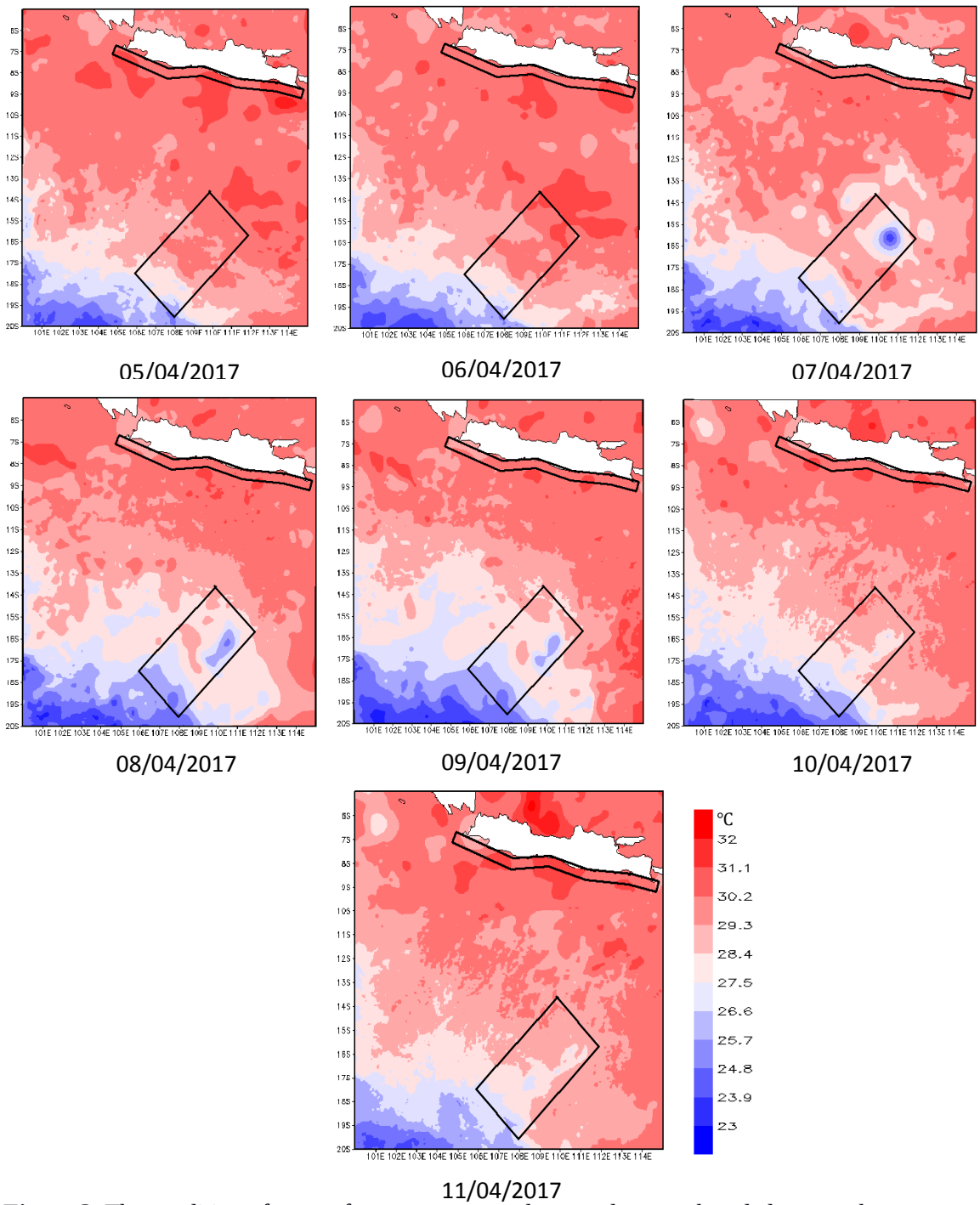

Figure 3. The condition of sea surface temperature along cyclone track and along southern coast area of Java island before the occurrence of tropical cyclone Ernie (5 April 2017) to the decayed phase of Ernie cyclone (11 April 2017). The condition of sea surface temperature expressed in Celsius (°C).

The condition of sea surface temperature in A2 region gave different response compared to A1 region. In general, the spatial distribution of sea surface temperature in A2 region tended to warm within the range of 30°C to 32°C and lasted for quiet long period since the occurrence of cyclone event to the end of the Ernie cyclone formation. The high value of sea surface temperatures in this region indicated a downwelling process. The wind that blows eastward along the southern coast of Java evoked surface currents leading to land which caused the mass of sea water along the coast pushed into its below deeper layers. This condition causes the mass of warm sea water to fill up the empty space in coastal areas [26].

3.3. The variability of chlorophyll-a concentration

Tropical cyclone activity contributes to the enhancement of vertical mixing and upwelling processes along the cyclone track. One of the parameters which closely related to this process is the variability of chlorophyll-a. Tropical cyclones could trigger the formation of eddy and upwelling processes that bring nutrient elements from the deeper layer and inject it into the surface layer [31]. The response of chlorophyll-a concentration on the A1 and A2 region due to the activity of Ernie cyclone can be seen in Fig. 4.

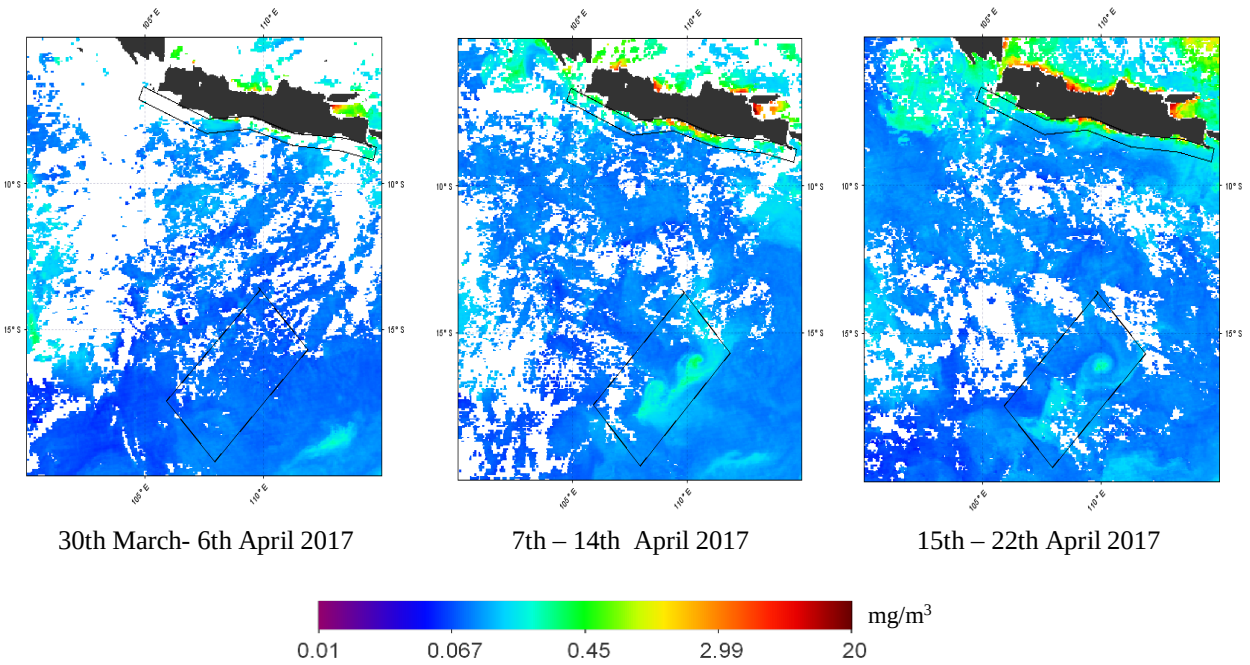

Figure 4. The 8-day composite data of chlorophyll-a variability in A1 and A2 region from 30 March – 22 April 2017.

This study used 8-day composite data of chlorophyll-a concentration. This is due to the incomplete data of daily chlorophyll-a concentration since there was a dense cloud cover in the tropical cyclone region. At the beginning period of the storm formation (30 March – 6 April 2017) based on Unisys Weather (table 1), it was clearly seen that the concentration of chlorophyll-a in A1 region was relatively low within the range of 0.08 mg/m^3 - 0.15 mg/m^3. The remote location of the tropical cyclone area from the coastal region and river estuaries made the contribution of soluble nutrient, usually produced by the river streams, was very low so that the chlorophyll-a concentration in this region was relatively low throughout the years.

During the cyclone period (7 - 14 April 2017), there was a significant increase in chlorophyll-a concentration in A1 region ranged between 0.15 mg/m^3 - 0.30 mg/m^3 and persisted for around 2 weeks throughout its post-cyclone period. The Ekman pumping mechanism allowed the water mass of rich-

nutrient from deeper ocean layer to rise into the surface of tropical cyclones. Therefore, there was an increase of chlorophyll-a concentration in A1 region after the occurrence of Ernie cyclone.

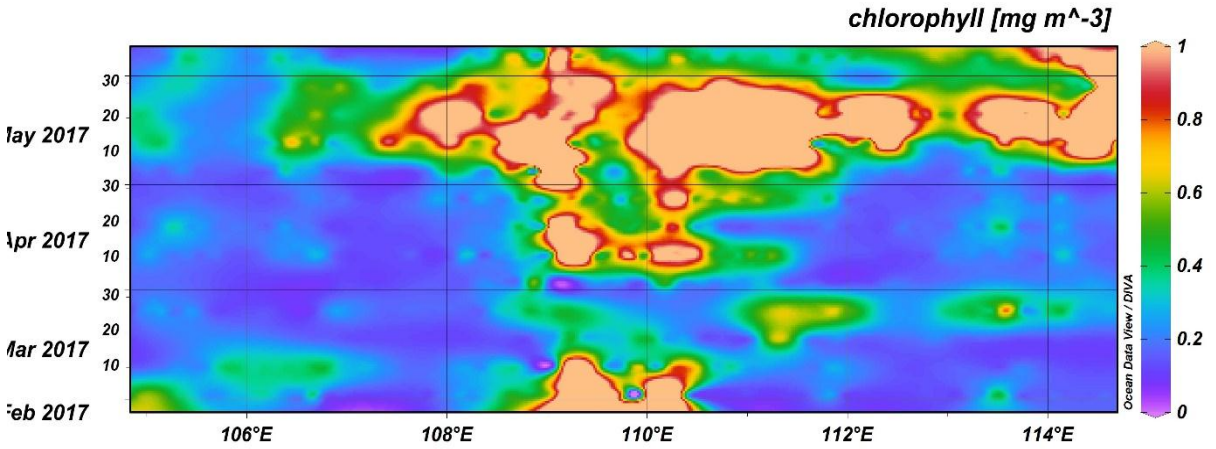

Figure 5. Variations of chlorophyll-a distribution on the southern coast of Java island (A2) before and after the occurrence of Ernie cyclone showed on the hovmoller diagram. The chlorophyll-a concentration expressed in mg/m^3.

Several related studies also showed that there is an increase of chlorophyll-a concentration along the cyclone trajectory. For instance, the concentration of chlorophyll-a was rose fivefold compared to the condition before the tropical cyclone LAM happened [22]. Meanwhile, the results of Ye et al., [32] showed that Nuri tropical cyclone was able to increase chlorophyll-a concentration five times higher than normal levels on the second day and continued nearly a week later.

However, the activity of Ernie cyclone gave different response to the variability of chlorophyll-a concentration in A2 region. The spatial and temporal distribution of chlorophyll-a in A2 region could be seen in the hovmoller diagram (Fig. 5). Before the occurrence of tropical cyclone, the overall chlorophyll-a concentration was quite low within the range of 0.1 mg/m^3 to 0.4 mg/m^3. The low concentration of chlorophyll-a was the impact of the changes in wind direction and ocean current patterns in A2 region which induced downwelling mechanism.

The concentration of chlorophyll-a in A2 region experienced a significant increase after the occurrence of tropical cyclone Ernie. Significant increase on the chlorophyll-a concentration after the occurence of Ernie cyclone due to the direction of sea surface wind which turned back into its normal condition (surface wind blow westwards in April), generated an upwelling process and triggered injection of colder sea water from deeper layer to the surface layer of the ocean [26]. Fig. 5 showed that the response of chlorophyll-a concentration in A2 region was quite slowly than that on the A1 region. It required considerable time (approximately one month after the Ernie cyclone happened) to induce significant increase in chlorophyll-a concentration in A2 region. This is because the wind speed in A2 region was much slower compared to the wind speed around the cyclone area (A1 region), therefore water mass transport mechanism in A2 region took longer times than that in A1 region.

4. Conclusions

The Ernie cyclone gave different effects on the area along the southern coast of Java island (A1) and along the cyclone trajectory (A2) area. The surface wind speed gradually increase along the cyclone track and decrease after the occurrence of cyclone. The increase in wind speed induced an Ekman pumping mechanism that caused the occurence of upwelling in A1 region. This upwelling process was characterized by a decrease in sea surface temperature, accompanied by a significant increase in chlorophyll-a concentration in A1 region. The activity of tropical cyclone Ernie caused westerly wind

pattern along the southern coast of Java. The eastwards wind pattern (wind flows from west to east) caused downwelling mechanism in the A2 region. This downwelling process was clearly showed by the high value of sea surface temperature and low chlorophyll-a concentration during the occurrence of tropical cyclone. Meanwhile, the wind direction pattern turned back into its normal, westwards wind pattern, after the occurrence of tropical cyclone Ernie. The westwards wind pattern (wind flows from east to west) led to the occurence of upwelling mechanism which can be identified by the increase of chlorophyll-a concentration in the A2 region after the occurrence of Ernie cyclone. This increase in chlorophyll-a concentration required longer time because the wind speed in A2 region was much more slower than that in A1 region, so that water mass transport mechanism in A2 region took longer time compared to that in A1 region.

Acknowledgments
We acknowledge Joint Typhoon Warning Center (JTWC) for providing basic data on the tropical cyclone events, NASA Jet Propulsion Laboratory (JPL) for providing Multi-scale Ultra-high Resolution Sea Surface Temperature (MUR SST) data, and NOAA for providing daily-average data of sea surface wind and 8-day composite data of chlorophyll-a concentration. Lastly, we thank Dr. *Endarwin*, S.Si, M.Si, Reynhard Syatauw, and Erwin Hayanata S.Sos for technical support and advice.

References
[1] Zhao, H., Tang, D., Wang, Y., 2008. *Comparison of phytoplankton blooms triggered by two typhoons with different intensities and translation speeds in the South China Sea*. Mar. Ecol. Prog. Ser. 365, 57e65.
[2] Shang, S., Li, L., Sun, F., Wu, J., Hu, C., Chen, D., Shang, S., 2008. Changes of temperature and bio-optical properties in the south China sea in response to typhoon lingling, 2001. *Geophys. Res. Lett.* 35 (**10**)
[3] Pan, J. and Sun, Y., 2013. Estimate of ocean mixed layer deepening after a typhoon passage over the south China sea by using satellite data. *J. Phys. Oceanogr*. 43 (**3**), 498-506.
[4] Zhao, H., Shao, J., Han, G., Yang, D., Lv, J., 2015. *Influence of typhoon matsa on phytoplankton chlorophyll-a off East China.* PLoS One 10 (9), e0137863
[5] Black, P.G., 1983. Ocean Temperature Changes Induced by Tropical Cyclones. Ph.D. *dissertation*. Pennsylvania State University, 278.
[6] Gopala Krishna, V.V., Murty, V.S.N., Sarma, M.S.S., Sastry, J.S., 1993. Thermal response of upper layers of Bay of Bengal to forcing of a severe cyclonic storm: a case study. *Indian J. Mar. Sci.* **22**, 8–11.
[7] Chinthalu, G.R., Seetaramayya, P., Ravichandran, M., Mahajan, P.N., 2001. Response of the Bay of Bengal to Gopalpur and Paradip super cyclone during 15–31 October 1999. *Curr. Sci.* 81 (**3**), 283–291.
[8] Babin, S.M., Carton, J.A., Dickey, T.D., Wiggert, J.D., 2004. Satellite evidence of hurricane-induced phytoplankton blooms in an oceanic desert. *J. Geophys. Res*. **109**, C03043.
[9] Chang, Y., Liao, H.-T., Lee, M.-A., Chan, J.-W., Shieh, W.-J., Lee, K.-T., Wang, G.-H., Lan, Y.-C., 2008. Multi-satellite observation on upwelling after the passage of Typhoon Hai-Tang in the southern East China Sea. *Geophys. Res. Lett.* **35**, L03612. http://dx.doi.org/10.1029/2007GL032858.
[10] Gierach, M.M., Subrahmanyam, Bulusu, Prasad, T.G., 2009. Physical and biological responses to Hurricane Katrina (2005) in a 1/25_ nested Gulf of Mexico HYCOM. *J. Mar. Syst*. **78**, 168–179.
[11] Lee, Chung I, Park, Mi-Ok, 2010. Time series changes in sea-surface temperature, chlorophyll a, nutrients, and sea-wind in the East/Japan Sea on the left- and right-hand sides of Typhoon Shanshan's track. *Ocean Sci. J*. 45 (**4**), 253–265.
[12] Stramma, L., Cornillon, P., 1986. Satellite observation of sea surface cooling by hurricanes. *J. Geophys. Res. **91***, 5031–5035.

[13] Suetsugu, M., Kawamura, H., Nishihama, S., 2000. *Sea Surface Cooling Caused by Typhoons in the Western North Pacific Ocean*. In: PORSEC proceedings, vol. 1. Goa, India, pp. 258–262.
[14] Lin, I.I., Wu, C.C., 2007. Typhoon-ocean interactions inferred by multisensor observations. *Recent Prog. Atmos. Sci.* 358.
[15] Babin, S. M., J. A. Carton, T. D. Dickey, and J. D. Wiggert. 2004. Satellite evidence of hurricane-induced phytoplankton blooms in an oceanic desert, *J. Geophys. Res*., **109**, C03043, doi:10.1029/2003JC001938.
[16] Oceans 109 (C3). Hung, C.C., Gong, G.C., Chou, W.C., Chuang, C.C., Lee, M.A., Chang, Y., Chuang, W.C., 2010. The effect of typhoon on particulate organic carbon flux in the southern East China Sea. *Biogeosciences J.* 7 (**10**), 3007e3018.
[17] Hong, C.H., Sohn, I.S., 2004. Sea surface in the East Sea with the passage of typhoons. *J. Korean Fish Soc*. 37 (**2**), 137–147.
[18] Kim, S.W., Yamad, K., Jang, L.H., Hong, C.H., Go, W.J., Suh, Y.S., Lee, C., Lee, G.H., 2007. Short-term variation of sea surface temperature caused by Typhoon Nabi in the Eastern Sea of Korean peninsula derived from satellite data. *J. Korean Fish Soc*. **40** (2), 102–107.
[19] D. Chen, L. He, F. Liu, and K. Yin, Effects of typhoon events on chlorophyll and carbon fixation in different regions of the East China Sea. Estuar. *Coast. Shelf Sci.*, vol. **194**, pp. 229–239, 2017.
[20] K. Muni Krishna and G. Song, Physical and biological changes in the south Bay of Bengal due to the Baaz cyclone. *Adv. Sp. Res.*, vol. **56**, no. 8, pp. 1658–1666, 2015.
[21] Enriquez, A.G., Friehe, C.A., 1995. Effects of wind stress and wind stress curl variability on coastal upwelling. *J. Phys. Oceanogr*. 25 (**7**), 1651–1671.
[22] Susilo, Eko., Hadianti, Sri., 2016. *Dapatkah Siklon Tropis Picu Peningkatan Konsentrasi Klorofil-A? (Studi Kasus : Siklon Tropis LAM).* Seminar Nasional Penginderaan Jauh, 972 – 980.
[23] Rayhan Nuris, J. L. 2015. Chlorophyll-a concentrations estimation from AQUAMODIS and VIIRS-NPP satellite sensors in south Java sea waters. *Int. J. of Remote Sensing and Earth Sciences Vol. **12** No. 1*, 63 - 70.
[24] Fadlan, Ahmad. Pengaruh Fenomena Monsun, El Nino Southern Oscillation (ENSO) dan Indian Ocean Dipole (IOD) terhadap Variabilitas Tinggi Muka Laut di Perairan Utara dan Selatan Pulau Jawa. M.S. *thesis*, Marine Science Dept., Diponegoro Univ., Semarang, Indonesia, 2017.
[25] Dietze, H., Löptien, U. 2016. Effect of surface current-wind interaction in eddy-rich general ocean circulation simulation of the Baltic sea. *Ocean Sci. J.* **12**: 977-986.
[26] Yoga, Bima, Raden. 2014. Dinamika *upwelling* dan *downwelling* berdasarkan variabilitas suhu permukaan laut dan klorofil-a di perairan selatan Jawa. *J. Oseanografi* (**3**):57-66
[27] Laing, A., and J. L. Evans, 2011: *Introduction to Tropical Meteorology. 2nd ed. University Corporation for Atmospheric Research*. [Available online at www.goes-r.gov/users/comet/tropical/textbook_ 2nd_edition/index.htm.]
[28] Ackerman, S. A., and J. A. Knox, 2015: *Meteorology: Understanding the Atmosphere. 4th ed. Jones and Bartlett Learning*, 575 pp.
[29] Cowan, R. M., Davies, E. L., Fairman Jr, J. G., Galarneau Jr, T. J., Schultz, D. M. 2015. *Revisting the 26.5°C Sea Surface Temperature Threshold for Tropical Cyclone Development*. American Meteorolgy Society. 1929-1943.
[30] Dare, R., dan Mcbride, J.L., (2011). The threshold sea surface temperature condition for tropical cyclogenesis. *Journal of Climate*, 24 (**17**):4570-4576.
[31] Wang, G., Ling, Z., dan Wang, C. 2009. Influence of tropical cyclones on seasonal ocean circulation in the South China Sea. *Journal of Geophysical Research*, **114**:1-9
[32] Ye, H.J., Sui, Y., Tang, D.L., dan Afanasyev, Y.D. 2013. A subsurface chlorophyll a bloom induced by typhoon in the South China Sea. *Journal of Marine Systems*, **128**:138145.